EXPERIENTIA

Vol. 24 – Fasc. 9 Pag. 865–976 15. 9. 1968

Self-Attenuation and Geometry in Single-Crystal Whole-Body Spectrometry. Application to Total Potassium Measurement in Man*

by G. JOYET and A. BAUDRAZ

Laboratory for Dosimetry and Protection, University of Zürich (Switzerland)

The earliest determinations of the whole body content of potassium on living humans were performed by SIEVERT in 1951–57[1,2], BURCH and SPIERS in 1954[3] and RUNDO in 1955[4] with high-pressure ionization chambers. In 1956, scintillation measurements of the 1.46 MeV γ-line of ^{40}K were made by ANDERSON[5] at Los Alamos National Laboratory using a 4π-liquid scintillation counter and by MARINELLI[6] and MILLER[7] at Argonne National Laboratory using an 8×4 inch NaI (Tl) crystal-detector. In 1958 BIRD and BURCH[8] introduced another scintillation method, using 3 large plastic detectors. Scintillation spectrometry of the ^{40}K γ-line appeared at the time when fallout from atomic weapon tests caused an increasing ^{137}Cs γ-line. The precise discrimination of these 2 γ-lines could not, of course, be done with ionization chambers.

After these measurements had been made, a large number of whole-body spectrometry facilities were built throughout the world. The characteristics of all of them up to the end of 1962 were described in a Symposium of the International Atomic Energy Agency[9]. About 80% of these installations were using one or more NaI (Tl) detectors, about 15% liquid or plastic scintillators, and only 4 were still using high-pressure ionization chambers (nitrogen or CO_2-filling at a pressure of 20–25 kg cm^{-2}).

Organic or *liquid scintillators*, because of their low cost, may be used in large volumes around the human body. Counting solid angles of up to 2π are common and as high as 4π have been achieved. The γ-ray detection efficiency is high and counting times may be reduced to a few minutes. These scintillators, however, have a low atomic number, so the Compton effect is large and the photopeak is negligible. The best half-resolution for the Compton distribution obtained at Los Alamos by LANGHAM, ANDERSON and DEAN[10] with a detector volume of 1600 l was 18% for ^{40}K and 25% for ^{137}Cs. Thus this method may be applied only in the measurement of a small number of widely separated γ-lines, e.g. for diagnostic work with known isotopes and especially for the measurement of potassium content in children. Up to the present time this system is not useful for radiation protection detection where a large number of unknown isotopes with low activity may occur.

Where both radiation protection investigations and medical measurements must be performed with the same equipment, whole-body spectrometry with *large NaI (Tl)-crystals* can be developed along the line initiated by MARINELLI[6] and MILLER[7]. The high atomic number of iodine gives a good photopeak ratio for such a crystal, e.g. 20% for ^{40}K and 26% for ^{137}Cs. Furthermore, the spectrometric resolution is good, i.e. as low as 6.6% for ^{40}K and 8% for ^{137}Cs. The small solid angle of about $\Omega/4\pi = 0.01$ (0.04π sr) for a crystal of 8×4 inches in a conventional geometry, see e.g. MILLER[7], may be compensated by a longer measuring time of 30–60 min. (Note that the measurement of ^{40}K by SIEVERT[1,2] with high-pressure ionization chambers required 3–4 h!)

* We would like to thank Prof. H. H. STAUB for his most valuable support and many helpful discussions, Prof. E. UEHLINGER for his help in supplying us with tissues, the Administration of the Hospital for much help, and finally Mrs. M.-L. JOYET for her constant technical collaboration. Special thanks go to Dr. and Mrs. R. W. BENJAMIN from Laboratory for Nuclear Physics of the Federal Institute of Technology for extensive revision of the manuscript.
The Swiss National Fund for Scientific Research financed all the equipment for the whole-body spectrometer.

1 R. M. SIEVERT, Ark. Fys. *3*, 337 (1951).
2 R. M. SIEVERT and B. HULQUIST, Br. J. Radiol., Suppl. *7*, 1 (1957).
3 P. R. J. BURCH and F. W. SPIERS, Nature *172*, 519 (1953).
4 J. RUNDO, J. Scient. Instrum. *32*, 379 (1955).
5 E. C. ANDERSON and W. H. LANGHAM, Science *130*, 713 (1959).
6 L. D. MARINELLI, Br. J. Radiol., Suppl. *7*, 38 (1957).
7 C. E. MILLER, Argonne National Laboratory Report ANL-5829, 144 (1957).
8 P. M. BIRD and P. R. J. BURCH, Physics Med. Biol. *2*, 217 (1958).
9 IAEA, *Directory of Whole-Body Monitors* (International Atomic Energy Agency, Vienna 1964).
10 W. H. LANGHAM, E. C. ANDERSON and P. DEAN, in *Directory of Whole-Body Monitors* (International Atomic Energy Agency, Vienna 1964), p. 401.

More recently, the small solid angle of irradiation of NaI (Tl) crystals is being increased by the use of multiple crystals around the body or 1 very large crystal. These developments are proceeding along 3 principal lines:

(a) NAVERSTEN[11] has used a scanning method of 2 crystals moving symmetrically above and below the mean plane of the extended body. This method involves a significant reduction of the effects of attenuation and inhomogeneous distribution of the γ-emitters in the body. However, for the measurement of natural radioactivity and for protection problems involving small contaminations, the counting time is not reduced significantly. This system is clearly more suitable for diagnostic work with relatively high activities.

(b) MORRIS et al.[12] at Oak Ridge Institute for Nuclear Studies have described an interesting system of 8 NaI (Tl) crystals arranged in 4 symmetrical pairs above and below the mean plane of a horizontally extended patient. The lack of sensitivity of 1 pair of crystals on an extended body is compensated by multiplication of fixed pairs. Further, the positioning flexibility of each pair of crystals, adaptable to the thickness of the body part which is 'seen' by each pair, is capable of counterbalancing the variation of attenuation with the different thicknesses of the body.

(c) In a standard chair or arc chair geometry all, or nearly all, parts of the body irradiate the single crystal simultaneously with about the same solid angle. The volume of the crystal, therefore, is fully utilized. With this geometry a very large single crystal may be used in order to increase the solid angle and thus the sensitivity. MAY et al.[13] have recently used this approach at Argonne National Laboratory with a NaI (Tl)-crystal $11^{1}/_{2} \times 4$ inches. In view of continuing advances in crystal manufacturing techniques, this clearly should not be considered an upper limit.

Semi-conductor detectors cannot be employed for whole-body spectrometry in spite of their excellent energy resolution. The solid angle and volume of these detectors are so small that the number of interactions per unit time would be far too low.

More complete historical reviews of the development of whole-body counting devices have been published by MARINELLI[14] and more recently (1964) by RAJEWSKY et al.[15] and by VENNART[16].

Limits and stability of the background reduction

In order to obtain the maximum reduction of the background (necessary for the measurement of potassium 40) we built a room similar to that of the Argonne Group[17], with a steel wall 18 cm thick. The work of RUNDO[18] and of MILLER[19] indicated clearly that steel shielding was to be preferred over lead shielding. Further, KOLB[20] and WELLER[21] showed recently that lead of different origin gave ^{210}Pb and ^{210}Po activity spans of 2 orders of magnitude (e.g. specific activities of 0.5×10^{-12} to 100×10^{-12} Ci g^{-1} Pb have been measured). In contrast to these results, the ANL-Group found that the specific activity of radium in old steel may be as low as 5×10^{-15} Ci g^{-1}. (We obtained a similar result with 3×10^{-15} Ci g^{-1}.)

Figure 1 shows 3 spectra corresponding to 3 steps of background reduction. Curve 1 shows clearly all the γ-lines of RaB and RaC. Air circulating with negative pressure in ducts, absorbed radon from the laboratory air and carried it into the steel room[22]. Improved ventilation with free air from outside and air-tight ducts with a positive pressure of 2 mm H_2O in the steel room reduced the background between 0.1 and 1.5 MeV by

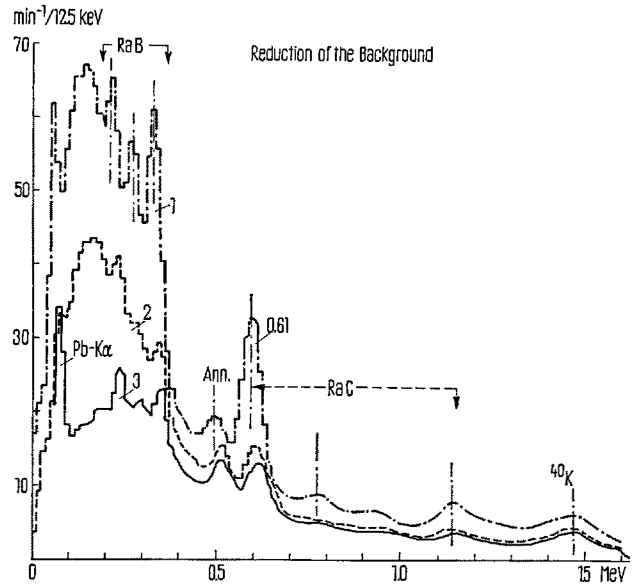

Fig. 1. Three steps of reduction of the background in the steel room: Curve 1, the laboratory air containing radon circulates through the room. Curve 2, the air comes from outside the building and circulates with positive pressure in the chamber. Curve 3, further reduction with 3 mm Boliden-lead coating.

[11] Y. NAVERSTEN, in *Clinical Uses of Whole-Body Counting* (International Atomic Energy Agency, Vienna 1966), p. 64.
[12] A. C. MORRIS, C. C. LUSHBAUGH, R. L. HAYES, H. KAKEHI and W. D. GIBBS, Oak Ridge Institute for Nuclear Studies Report ORINS-49, 111 (1964).
[13] H. A. MAY, O. J. STEINGRABER and P. E. HESS, Argonne National Laboratory Report ANL-7220, 39 (1965–66).
[14] L. D. MARINELLI, Proc. XIth Int. Congr. Radiol., Rome 1965, p. 1291.
[15] B. RAJEWSKY, A. KAUL and J. HEYDER, in *Assessment of Radioactivity in Man* (International Atomic Energy Agency, Vienna 1964), vol. 1, p. 15.
[16] J. VENNART, Nature *204*, 1041 (1964).
[17] G. JOYET and A. HAUPTMANN, Z. angew. Math. Phys. *16*, 547 (1965).
[18] J. RUNDO, in *Directory of Whole-Body Monitors* (International Atomic Energy Agency, Vienna 1964), p. 321.
[19] C. E. MILLER, in *Directory of Whole-Body Monitors* (International Atomic Energy Agency, Vienna 1964), p. 381.
[20] W. KOLB, Hlth Phys. *12*, 1823 (1966).
[21] R. I. WELLER, Hlth Phys. *12*, 1823 (1966).
[22] The laboratory has thick walls of arkose with granitic component.

50% (curve 2). A 3 mm Boliden-lead lining of the room brought a further reduction of 30% in the same energy range (curve 3). This lining absorbs the low-energy γ-rays from multiple scattering in the steel wall of high-energy γ-rays coming from outside. The absorption in lead induces the excitation of the K_α-lines of 72.8 and 75.0 keV[23].

Figure 2 shows the background, after all improvements, measured with the conventional NaI (Tl)-crystal of 8 × 4 inches. Measurements have shown that the RaB (0.24 MeV), the RaC (0.61 MeV) and the ^{40}K (1.46 MeV) γ-lines originate entirely in the three 6363′ phototubes[24].

It is possible to calculate the energy flux due to ^{40}K and the higher-energy radiation from RaC which comes through the 18-cm steel walls. For this calculation it was necessary to make a measurement of these γ-lines outside of the shielded room with the same detector, and freely to take into consideration the build-up factors[25]. This flux is at present 50 MeV min^{-1} and could be reduced to 8 MeV min^{-1} by a steel wall 24 cm thick. Further, the continuous spectrum derived from the activity of the phototubes is 95 MeV min^{-1}. Thus, with this shielding technique, the use of inactive phototubes and an increase of the steel thickness to 24 cm, a reduction of about 30% in the background could be achieved. The 'background index' which is now 0.26 min^{-1}/cm^3 should then fall below 0.20.

The *stability of the background* of the chamber was observed repeatedly in different weather conditions, each time with a 600 min measurement. The mean values with their extreme variations are given in Table I in the energy ranges 0.1–1.5 and 0.1–2.0 MeV.

These variations are very low, no more than ± 1.5% in both energy ranges. Nevertheless, a slight reduction appears with rain and wind when the soil is moist and able to retain the radon produced. With dry soil and no wind, a slight rise of the background is evident. We ascribe this low and negligible variation of the background to the effective filtration of the air admitted to the steel room and particularly to the electrostatic filter which carries off a great deal of the ionized active decay products of radon. In addition, the reduced radon transit time of 5 min in the chamber does not permit the build-up of a noticeable quantity of short-lived decay products of Rn.

The same Table shows that the variation of the background in the ^{40}K window of 250 keV-width is completely negligible.

First measurements on man with the standard 'Tilting chair'

The single crystal subject-detector geometry introduced by Marinelli and May was adopted, in view of its simplicity and its comfort for the subject, for our first design 4 years ago (Figure 8a). Suspecting that body shape and size could be an important factor for the calibration, we systematically measured each person's weight and height and his circumference at 3 points: around the hips, waist and chest. The mean value $\overline{P}$ of these last 3 quantities was calculated. The height, weight and $\overline{P}$ clearly give some idea of the shape of the body. The relative activity under the photopeak of ^{40}K was counted for 30 min, using 128 channels and 12.5 keV/channel.

We first examined the relative activity/kg gross weight of 37 normal men of 21–47 years of age as a function of $\overline{P}$ and found a strong dependence on this parameter. Between $\overline{P}$ = 78 cm and $\overline{P}$ = 104 cm, the relative specific activity shows a drop of as much as

Table I. Variation of the background with weather

Weather	Energy band		^{40}K-window
	0.1–1.5 MeV min^{-1}	0.1–2.0 MeV min^{-1}	250 keV min^{-1}
Rain with wind	792 ± 4	844 ± 4	59.0 ± 0.4
Rain without wind	800 ± 3	852 ± 3	59.8 ± 0.7
Soil frozen, no wind	805 ± 5	854 ± 6	59.4 ± 1.2
Soil dry, 5–18°	808 ± 7	860 ± 7	60.1 ± 1.2

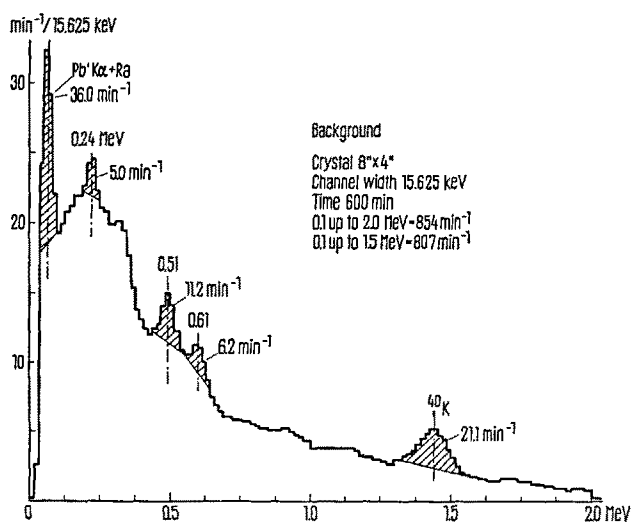

Fig. 2. Background after all improvements.

[23] An increase of the lead lining from 3–6 mm reduced the background by only a further 7%. In order not to put too much lead with its higher specific activity in the room, a lining from 4–5 mm lead seems to be an optimum solution. A supplementary lining of 10 mm steel put above the lead layer will remove the lead K_α-lines.

[24] RCA C 70 145 phototubes are now available with very low activity, the relative activity for 3 tubes being as low as 3 min^{-1} in the photopeak of ^{40}K.

[25] H. Goldstein and J. E. Wilkons, U.S. Atomic Energy Commission Report NYO-3075, NDA Report 15C-41 (1954).

39% [26]. It can be shown that the drop is not a systematic consequence of age.

Suspecting the influence of body *fat*, we took into account the *normal weight* given, as a function of the height, by the Life Extension Institute of New York City [27]. We did not correct all weights, but only those where the difference between theoretical and gross weight was at least 6 kg. The 'corrected weight', which had to be taken for 18 subjects, was the average between 'true' and 'normal' weight. (This procedure of limited correction is based on the fact that, when fasting, obese patients lose weight and potassium at the same time and that the 'normal' weight, which is determined by height only and makes no allowance for the different morphologies of the body (i.e. asthenic, athletic, pyknoid types), is a very rough estimate.)

In Figure 3 the new relative specific activity/kg is plotted against the average perimeter $\overline{P}$. The correction gave a substantial reduction of the slope of the average straight line drawn through the points (a fall of 15% only between $\overline{P} = 78$ and $\overline{P} = 104$ cm). This correction is thus indispensable, but not completely sufficient. Further, the dispersion on both sides of the straight line is high, amounting to about 20%. If we plot the same corrected specific activity against the weight (corrected as above), we again find a slope of about 10% between 60 and 80 kg. Using a whole-body counter with 8 plastic detectors, TAUXE at Mayo Clinic [28] found a similar variation of the ^{40}K specific activity with weight. Therefore, it became necessary to study thoroughly the problems of self-attenuation and geometry in the crystal-subject system.

Self-attenuation and geometry in a single-crystal system

Only 2 authors appear to have undertaken calculations taking into account both geometry and self-attenuation for the crystal-subject system. NAVERSTEN [11] studied the variation of the total efficiency as a function of depth considering both geometry and attenuation effects for 2 detectors in a scan-bed system for a phantom 20 cm thick homogeneously filled with ^{137}Cs. GENNA [29] similarly devised an analytical method in the scanning-bed geometry for the determination of the response of a hypothetical radioactive band lying at a known depth of the phantom. We are studying here not the scanning-bed geometry but a single crystal-chair geometry, which we shall show allows a simple and general solution for a large energy range.

We consider first a homogeneous distribution of the γ-emitter in the body. This is roughly the case for some isotopes such as ^{40}K and ^{137}Cs, which are present in approximately equal concentrations in all tissues with the exception of bones and fat. For some other isotopes which are injected i.v., the distribution may be considered as homogeneous during a certain time after the injection, vis. during the intravasal and extra-cellular phase of the isotope. For both these cases calibration for homogeneous distribution is of great importance.

As shown in Figure 4, we consider a cylindrical volume of 1 cm² section in a homogeneous radioactive layer of thickness $D - d$. An elementary volume of thickness dx irradiates the crystal in the solid angle $\Omega/4\pi$. D is the fixed distance between the bottom of the radioactive layer up to the average depth Δ in the crystal, where the first collision occurs. We apply the following definitions in the calculation:

a, R = height and radius of the NaI (Tl) crystal;

x = distance between the elementary volume $1 \cdot dx$ up to the depth Δ in crystal;

A = specific activity of the layer with a density equal to 1.0;

ν = frequency of the emitted γ-line;

F = photofraction of all the collisions in the crystal;

μ_0^c = total attenuation coefficient in the crystal;

μ_0^w = total attenuation coefficient in the active layer (water);

$(1 - e^{-\mu_0^c a})\, F$ = proportion of all the γ-rays crossing the crystal and giving a primary or secondary photoeffect;

M = relative activity (measured in the photopeak) per unit volume of active layer.

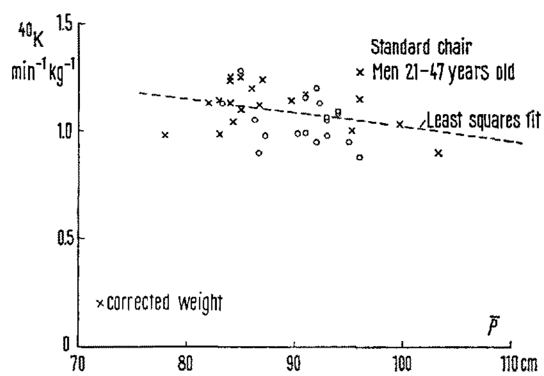

Fig. 3. Relative specific activity of ^{40}K plotted against the average perimeter $\overline{P}$. ×, corrected weight for excess or lack of fat.

[26] G. JOYET, Z. angew. Math. Phys. *16*, 849 (1965).
[27] *Documenta Geigy, Wissenschaftliche Tabellen* (Basel 1955), p. 247.
[28] N. TAUXE, Mayo Clinic Proc. *41*, 18 (1966).
[29] S. GENNA, in *Clinical Uses of Whole-Body Counting* (International Atomic Energy Agency, Vienna 1966), p. 37.

For the elementary volume $dx \cdot 1$, the relative activity measured in the photopeak is

$$A\, \nu\, (1 - e^{-\mu_0^c a})\, F\, \frac{\Omega}{4\pi}\, e^{-\mu_0^w (x-d)}\, dx \cdot 1 .$$

Considering the solid angle

$$\frac{\Omega}{4\pi} \cong \frac{\pi R^2}{4\pi x^2} \cong \frac{S}{4\pi x^2}$$

we have for the relative specific activity

$$\boldsymbol{M} = A\, \boldsymbol{G}_p\, \boldsymbol{A}_a \tag{1}$$

with

$$\boldsymbol{G}_p = \frac{\nu\,(1 - e^{-\mu_0^c a})\, F\, S}{4\pi} \tag{2}$$

and

$$\boldsymbol{A}_a = \frac{e^{\mu_0^w d}}{D-d} \int_d^D \frac{e^{-\mu_0^w x}}{x^2}\, dx . \tag{3}$$

By partial integration,

$$\boldsymbol{A}_a = \frac{e^{\mu_0^w d}}{D-d} \left\{ \left(\frac{e^{-\mu_0^w d}}{d} - \frac{e^{-\mu_0^w D}}{D} \right) - \mu_0^w \int_d^D \frac{e^{-\mu_0^w x}}{x}\, dx \right\} . \tag{4}$$

This factor is dependent on the fixed distance D from the bottom of the active layer to the crystal, the thickness $D-d$ of this layer and the total attenuation coefficient μ_0^w. Thus it is justified to call it *self-attenuation factor* $\boldsymbol{A}_a$.

The factor $\boldsymbol{G}_p$, which is proportional to the number of photoeffects for all the γ-rays crossing the crystal may be called *geometrical* and *photo factor* $\boldsymbol{G}_p$.

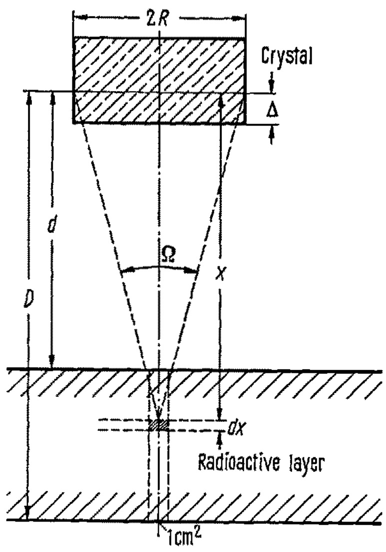

Fig. 4. Schema for calculation of self-attenuation.

The relative specific activity $\boldsymbol{M}$ measured in the photopeak, is proportional to the specific activity A and would be independent of the thickness $D-d$ of the active layer if it were possible to build a geometry subject-detector where both factors $\boldsymbol{A}_a$ and $\boldsymbol{G}_p$ were constant. Thus we will study these 2 factors separately below.

Dr. ing. K. BAUKNECHT of the Institute for Operation Research has been kind enough to calculate with an IBM 1620 computer several values of the self-attenuation factor $\boldsymbol{A}_a$ (Eq. 4) for the ^{137}Cs (0.662 MeV) and ^{40}K (1.46 MeV) γ-lines. The results of these calculations are given graphically in Figures 5 and 6. In these Figures the values of $\boldsymbol{A}_a$ are given for some fixed distances D (50, 53, 55, …, 75 cm) against the thickness $D-d$ of the active layer. We see that for short distances of D (50–55 cm), the variation of the self-attenuation $\boldsymbol{A}_a$ with layer-thickness is very substantial, e.g. 20–30% in the usual range thickness of 12–26 cm. If in the same thickness range we take a greater and fixed distance D crystal-layer of 65 cm, we see that the extreme variations of $\boldsymbol{A}_a$ amount to 3.5% for ^{40}K and 2.5% for ^{137}Cs (Figures 5 and 6).

Thus, the first conclusion is that the distance D, i.e. the distance from the fixed support of the active layer up to the crystal, must be theoretically about 65 cm, and the commonly used distances of 50 cm or less are not acceptable for the measurement of homogeneous radioactive distribution with 1 crystal.

We now consider the *geometrical and photo factor* $\boldsymbol{G}_p$ (Eq. 2). This factor is constant for a fixed γ-emitter

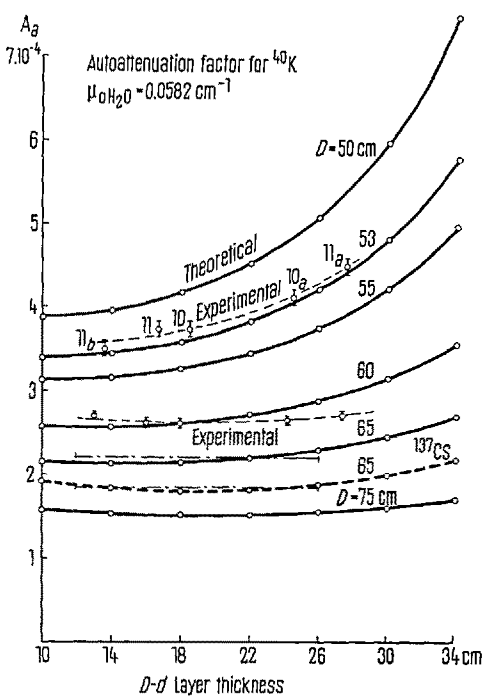

Fig. 5. Theoretical and experimental self-attenuation factors $\boldsymbol{A}_a$ for ^{40}K (1.46 MeV).

source put on the axis of the cylindrical crystal. But if the source moves *around* the crystal in the coaxial plane of the crystal, the collision term $(1 - e^{-\mu_0^c a})$ and the surface S will both vary. The calculation of G_p for a non-coaxial source is very complex, and it is easier to determine a curve experimentally which gives a constant value for G_p in a coaxial plane. This is shown in Figure 7. In an effort to achieve a constant response in the photopeak for each γ-line, we placed point sources of ^{137}Cs and ^{60}Co (the 1.33 MeV γ-line) at different azimuths 0°, 15°,..., 180° and different distances *around* the crystal. The interpolation for a fixed azimuth was made with the inverse-square law of distance. Figure 7 shows 2 concentric dotted curves with constant response for the 0.662-MeV γ-line and 1 solid curve for the 1.33-MeV γ-line. We see that the radial differences between the external ^{137}Cs-curve and the 1.33-MeV curve are very small, no more than 1.5 cm. Thus the same profile may be applied in a large energy range from about 0.6 MeV to about 1.5 MeV. We used as a profile the isotropic response curve of 1.33 MeV since this energy is near the 1.46 MeV of the ^{40}K line. It is apparent that this profile

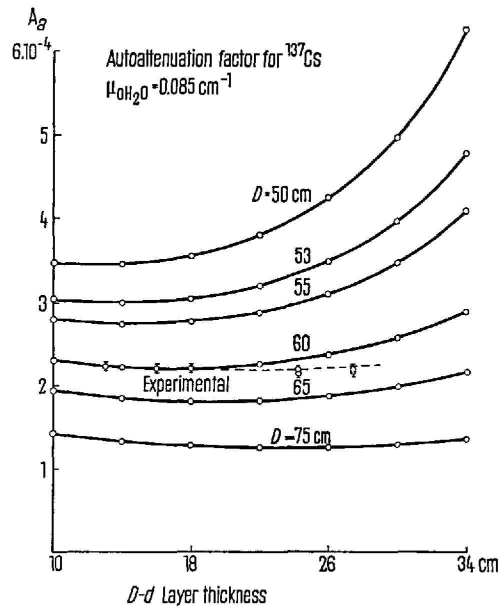

Fig. 6. Theoretical and experimental self-attenuation factors A_a for ^{137}Cs (0.662 MeV).

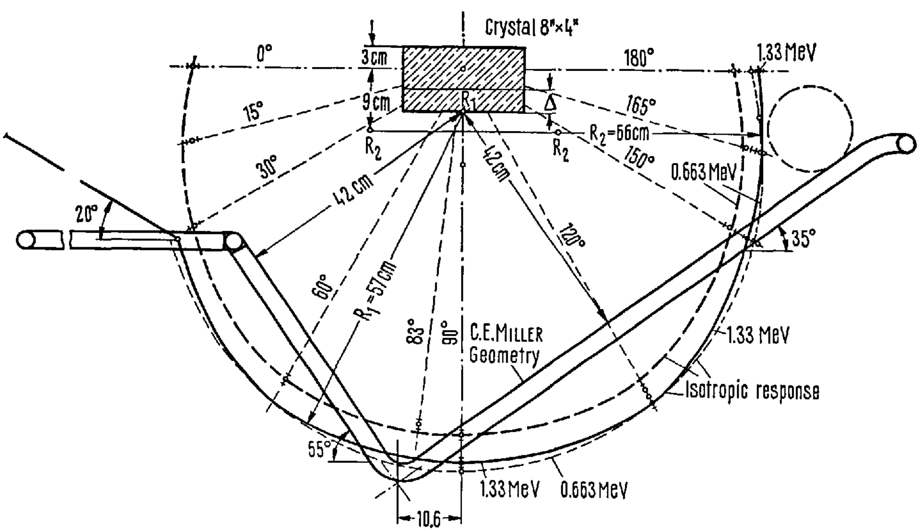

Fig. 7. Curves of isotropic response for point sources of ^{137}Cs (0.662 MeV) and ^{60}Co (1.33 MeV).

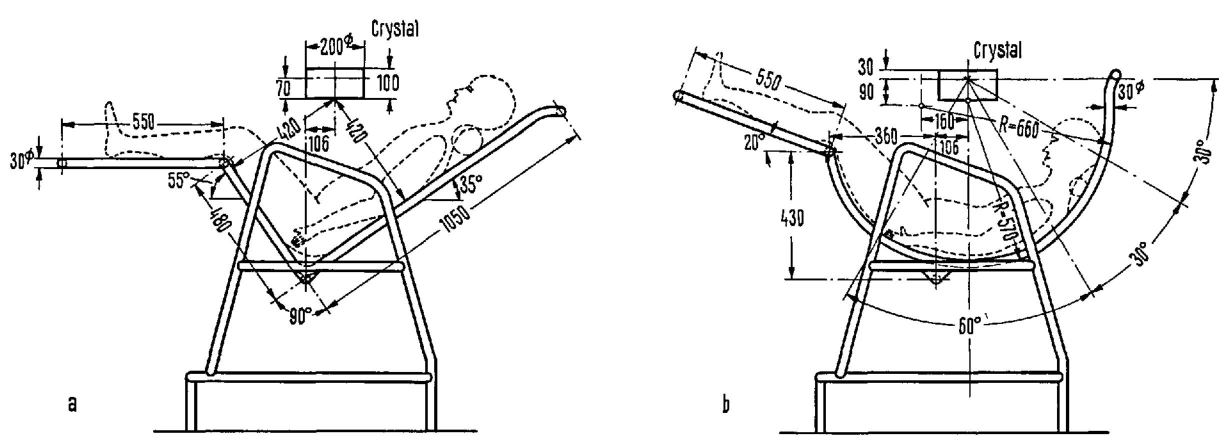

Fig. 8. (a) Profile of the standard chair. (b) Profile of the new quasi-elliptical chair.

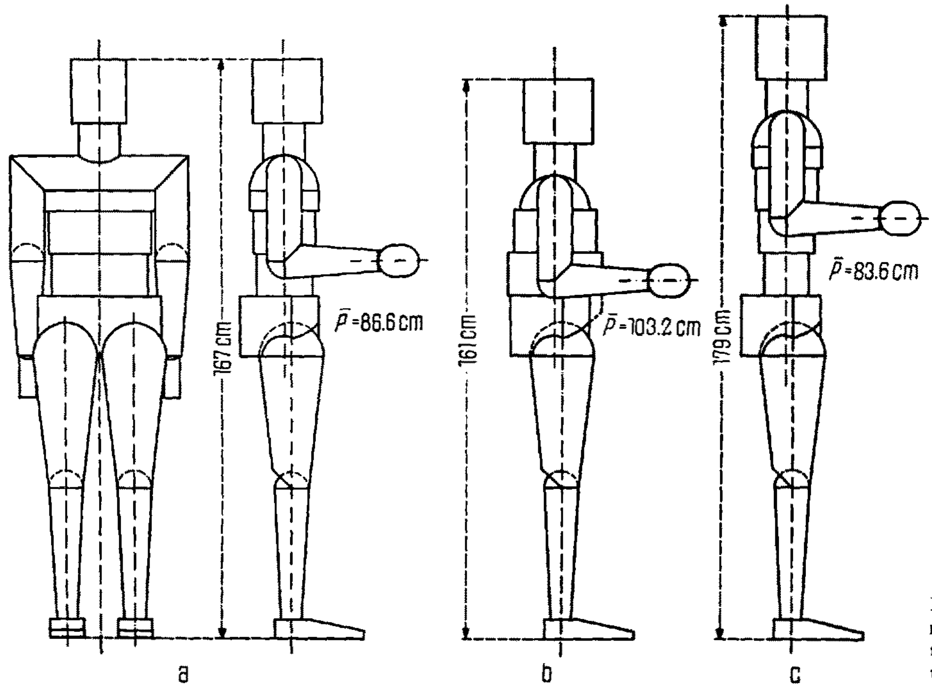

Fig. 9. (a) Phantom of the standard man (face and profile). (b) Phantom of the plump, short man. (c) Phantom of the slim, tall man.

may be drawn with 2 arcs of 57 cm and 66 cm radius respectively (the last being excentric) joined by an approximation line. The construction of a chair in steel tubing of 30 mm diameter is shown in Figure 8b. The subject lies in a comfortable position in the quasi-elliptical chair, which can also be made to see-saw.

Experimental response of the new chair with quasi-elliptical profile. Phantom calibration.

We have shown (Eq. 1) that the relative activity M measured in the photopeak is independent of the thickness $(D-d)$ of the active layer, provided that the geometrical factor G_p and the self-attenuation factor A_a may be maintained constant. The quasi-elliptical profile of the chair ensures a fairly constant value of G_p. But for A_a the calculation was made for a cylindrical layer coaxial to the crystal. Since different sections of the body such as trunk, legs and head have a form very different from that of a coaxial cylinder, it was necessary to check experimentally the extent to which the theoretical variation of A_a, given by Figures 5 and 6 for different distances D, is applicable to different sections of the body.

With the help of A. HAUPTMANN, dipl. phys., we built phantoms composed of 14–18 separable and exchangeable containers to reproduce different physical types: a *standard man* (Figure 9a), a *plump and short man* (Figure 9b), and a *slim and tall man* (Figure 9c). These containers were made of Peraluman 30 sheets, 1.2–1.5 mm thick[30]. They were filled with calibrated radioactive solutions of ^{137}CsCl or KCl with an additive of $Na_2Cr_2O_7 \cdot 2H_2O$ in order to avoid electrolysis and hydrogen production at the surface.

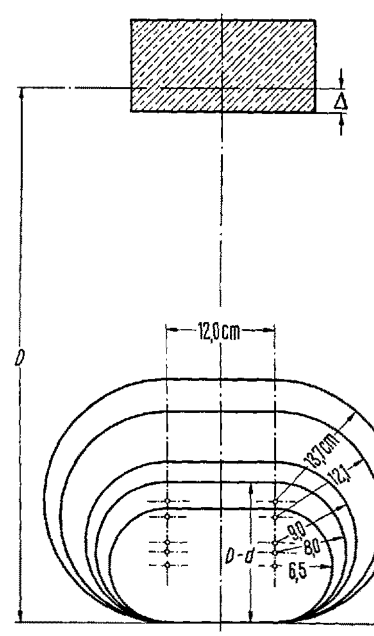

Fig. 10. Cylindrical containers of different cross-section put under the crystal at a distance D.

As shown in Figure 10, cylindrical containers representing different sections of the thorax and filled with KCl solution were put under the crystal at 2 distances D: 52.5 and 60.0 cm. We see in Figure 5 that the 2 experimental curves agree surprisingly well with the theoretical ones. For $D = 60.0$ cm we see that the variation

[30] Constructed by Mecaplex in Granges, Switzerland.

of the experimental value of A_a for body thickness of 13–27 cm is not more than $\pm$ 2% of the average value. A similar experiment was made with the same containers filled with $^{137}CsCl$ and put at a distance $D = 60.0$ cm from the crystal. The experimental curve is shown in Figure 6. It is somewhat different from the theoretical curve, the minimum being moved to the right side, but it is flatter and the extreme deviations are only $\pm$ 3% in the thickness range $D - d$ of 13–27 cm.

The theory of self-attenuation factor A_a was developed for an irradiation of the crystal in the azimuth 90°, so it was necessary to check experimentally how the measured specific activity varied with the azimuth at 0° or 180°. The same containers were placed horizontally and symmetrically to the horizontal symmetry plane of the crystal at an average distance of 50 cm. The relative activity per unit volume between phantom thickness of 13–24 cm showed extreme deviations of only $\pm$ 3%. In conclusion, we may assume that the self-attenuation theory developed for a cylinder coaxial to the crystal is applicable to sections of the trunk of very different sizes placed at different azimuths of the crystal.

The detector response for each piece of the phantom of the *normal man* put at its own position in both the standard chair and the new quasi-elliptical chair was measured and is given for ^{40}K in Table II.

The advantage of the new elliptical geometry of the chair is that it gives a practically constant response/g potassium for each piece of the phantom (lower legs and feet are obviously excluded). The differences in comparison with the standard chair are especially striking for head, abdomen, hips and thighs.

Calibrations for men of different shapes were made with help of the phantom pieces shown in Figures 9 a–c, each piece being filled with a calibrated solution of KCl, $^{137}CsCl$ or ^{131}I. The result is given in Figure 11 as a function of the average perimeter $\bar{P}$. The window widths of the photopeaks were 250 keV for the 1.46-MeV γ-line, 150 keV for the 0.662-MeV line and 106 keV for that of 0.364 MeV[34]. Figure 11 shows for ^{137}Cs and ^{40}K the slow decrease of the calibration constant with the increase of $\bar{P}$: the total decrease in the whole calibration range was only 6% for each of the 2 nuclides[31]. In the same Figure, the maximum total decrease of calibration for ^{131}I in the same perimeter range is 8%. With a larger crystal (i.e. 35 × 18 cm), D could be reduced down of 10% without modification of the horizontal half-axis of the chair. The calibration curves then could be practically horizontal (slope zero).

A spectrum of the standard phantom is depicted in Figure 12 for ^{137}Cs. The spectrum of a ^{137}Cs point source[32] is added in order to compare the Compton spectra occurring in the crystal and in the thickness of the phantom respectively. For each curve, the Compton spectrum is integrated above 0.05 MeV to the upper limit of the photopeak as well as under the photopeak. For ^{137}Cs the ratio of the photopeak to the Compton plus photopeak is 0.58_5 for the point source and is only 0.25_6 for the phantom. Thus, for the same intensity in the photopeak, 33% of the registered γ-rays are to be attributed to scattering in the phantom itself. The photopeak ratio varies from 24–26% for ^{137}Cs and from 19–20% for ^{40}K for the slim man and the corpulent man respectively. These are very slight variations.

In Figure 13 the spectra from 2 measurements on the standard phantom, one with ^{137}Cs and one with ^{40}K, are combined in order to obtain the complex spectrum of a phantom measured for 300 min. As can be seen, at the left of the maximum energies of recoil electrons (*Co*) for ^{40}K and ^{137}Cs are 2 shoulders which are not to be

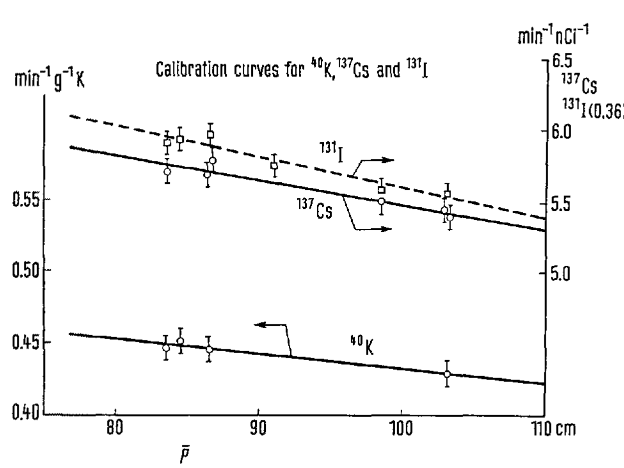

Fig. 11. Calibration curves plotted against the average perimeter of the thorax $\bar{P}$. The slope of the curves could be brought down to zero with a larger crystal (i.e. 35 × 18 cm) and a reduction of 10% for D.

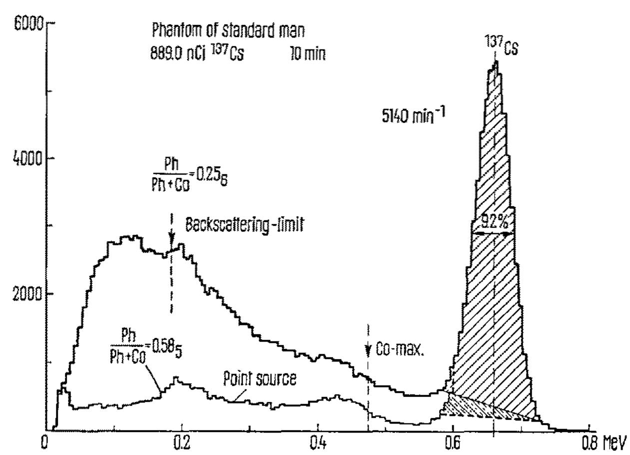

Fig. 12. Spectrum of phantom of the standard man filled with a ^{137}Cs solution, compared with the spectrum of a point source 'in air'.

[31] For each person we consider these variations of the calibration against $\bar{P}$.

[32] The point source was put at a distance of 60 cm on the axis of the crystal 'in air' 58 cm above the steel and lead floor.

ascribed to γ-lines. The 2 backscattering-limits in the neighbourhood of 0.2 MeV give such a shoulder.

The phantom spectrum of Figure 13 must be compared with the spectrum of a normal man in Figure 14, taken for 45 min (scale of ordinate 10^3). This man, 171.5 cm tall, with a weight of 64.8 kg and an average perimeter of 89.2 cm, has a potassium weight of 145 g and a ^{137}Cs-activity of 14.7 *nCi*. With these values it is possible to calculate some points for the total Compton continuous spectrum of a standard phantom containing 145 g K and 14.7 *nCi* ^{137}Cs. The points calculated are plotted o in Figure 14. Taking into account the statistical fluctuation, it is apparent that from 0.15 MeV upwards the spectrum of the man exactly fits that of the phantom containing only ^{137}Cs and ^{40}K. The RaC' γ-line of 1.12 MeV is not discernible, but in the neighbourhood of 0.1 MeV the spectrum of the phantom clearly does not rise as high as that of the man. Some unknown isotopes, probably ^{144}Ce and further ^{90}Sr-^{90}Y are present in the body.

Calculation of low-activity photopeaks

The measured spectrum of a normal young man shown in Figure 14 covers an energy range of 1.6 MeV with a channel width of 12.5 keV and a counting time of 45 min[33]. The background, which was recorded negatively in the analyzer memory during an equivalent 45-min live time, has been subtracted. Note that in low count regions of the spectrum statistical fluctuations may cause negative counts to appear on the display after background subtraction. For graphical display,

Table II. Specific response of the different pieces of phantom in standard and new chair

Pieces of the phantom	Weight of solution (kg)	Relative activity			
		'Standard chair'		New chair	
		min^{-1}/ g K	% of total	min^{-1}/ g K	% of total
Head + neck	6.63	0.35_5	58.7	0.48_3	$101._8$
Shoulders + upper part of lungs	9.94	0.57_0	94.3	0.46_9	$98._7$
Under part of lungs + abdomen	10.67	0.71_9	119.0	0.47_9	$100._7$
Pelvis and hips	7.91	0.55_1	91.2	0.47_7	$100._2$
Thighs	15.84	0.67_9	112.4	0.47_0	$98._7$
Arms and hands[a]	7.51	0.59_5	98.5	0.47_6	$100._0$
Total (without legs and feet)	58.49	0.60_4	100.0	0.47_6	$100._0$
Legs and feet	6.61	0.27_1	47.6	0.21_0	$46._2$
Containers weight (Al)	9.18	–	–	–	–
Total weight of filled phantom	74.28	0.57_0	–	0.45_5	–

[a] The elbows are sustained 5 cm above the profile of the new chair.

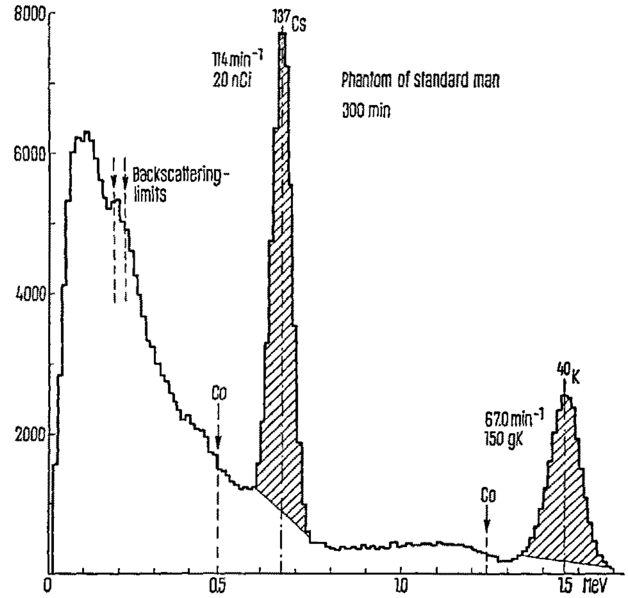

Fig. 13. Spectrum from the phantom of the standard man filled with 20 nCi ^{137}Cs and 150 g of potassium.

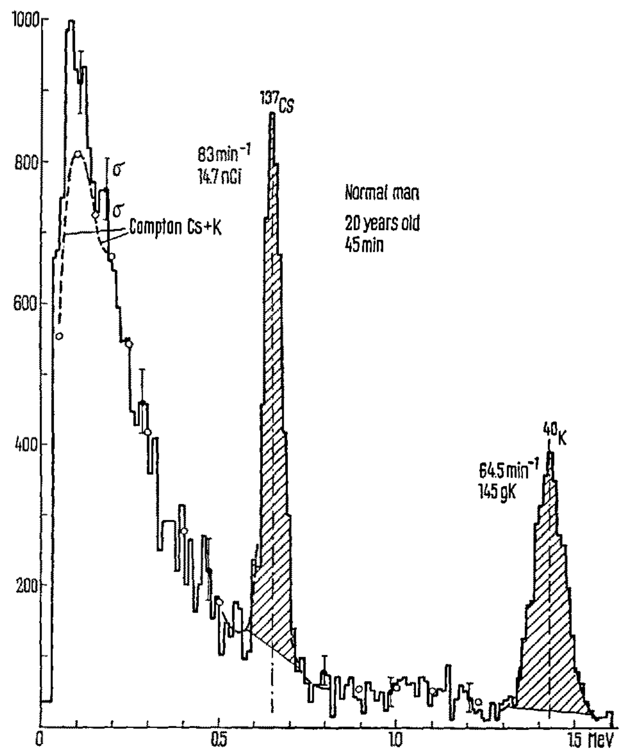

Fig. 14. Measured spectrum of a normal young man in Zürich, spring 1967.

[33] Measurements were made originally in the energy range 0–2.0 MeV in order to record the 1.76-MeV γ-line of RaC. We reduced the range to 1.6 MeV after having seen that the 1.12 MeV-line of the RaC appeared with about the same intensity in the photopeak as the 1.76-MeV line.

5–30 counts are added to each channel *after* the data has been recorded for analysis.

Because of the low intensities of the measured activities and the high statistical fluctuations in each channel the photopeaks, particularly that for ^{40}K, do not appear as good theoretical Gaussian distributions. Further, because of scattering in the tissues the curve is no longer symmetrical, and a trapezoidal base should be subtracted from the photopeak window. The statistical error involved in the subtraction of the base can be reduced in the following manner. The width of the window is $2\,(E_w - E_\gamma)$ as shown in Figure 15. We take on each side of E_w narrow energy bands ΔE_1 and ΔE_2, which are related by the equation

$$(\Delta E_1 + \Delta E_2)\, f\,(E_w) = \int_{E_w - \Delta E_1}^{E_w + \Delta E_2} f\,(E)\, dE \qquad (5)$$

which makes the 2 hatched surfaces in Figure 15 of equal area. The function $f\,(E)$ is the normal Gaussian distribution and its integral can be found in the Tables. In Eq. 5 the window width, $2\,(E_w - E_\gamma)$, is chosen large enough so that the higher limit of the integral is always 0.500. The window width being determined, at each value of ΔE_1 corresponds a fixed value of ΔE_2. For ^{40}K, the resolution is 6.3% and we take a window width of 250 keV; if $\Delta E_1 = 18.75$ keV ($1^1/_2$ channels) then $\Delta E_2 = 35.8$ keV (about 3 channels). Thus the 2 limits of the trapezoidal base are defined $1^1/_2$ channels inside and 3 channels outside of the window edge. A detailed calculation is carried in Table III for the spectrum of Figure 14. The values of the last 32 channels are given between 1.2 and 1.6 MeV.

The position of the axis ¦ of the photopeak is determined from the spectrum (see e.g. Figure 14, the numerical values are given in Table III). The edges of the window are denoted [ ] and on both sides of these edges $1^1/_2$ and 3 channels, respectively, are marked off ( ). Taking account of the channels divided by 2, we obtain

Sum of the 20 channels (window width)		3436
Trapezoid to be subtracted	$^{20}/_9 \times 240 =$	533
	Difference	2903

Since the counting time was 45 min, we have a ^{40}K relative activity of 64.5 min^{-1}. To the average perimeter $\overline{P} = 89.2$ cm corresponds, according to Figure 11, a calibration value of 0.44_4 min^{-1}/g K. The subject thus has a potassium weight of 145 g, i.e. with nearly normal weight of 64.8 kg a concentration of 2.24 g K/kg.

This improvement in the calculation reduces the standard deviation of potassium determination of 2%, i.e. to 3.5–5.5% for the man and to 5.5–7.5% for the woman.

On each spectrum of man the ^{137}Cs peak arising from the fallout of atomic weapons appears. The activity is determined by calculating the area under the peak with a window width of 150 keV[34].

Table III. Calculation of low activity photopeak

MeV	—	—	—	—	—	—	—	—
1.2	44	24	30	13	14	3(9	14	38
	4[2	49)	31	73	127	174	181	290
	317	360	39¦1	350	275	259	200	133
1.5	82	63	36	(18	1]2	17	18	2)5

The total potassium in 20-year-old men and women

With the technique and the calculation method described, we measured each time 2 groups of about 50 young men and 50 young women 20 years of age, in spring 1966, autumn 1966 and spring 1967. The men were recruits measured with the kind permission of the Army Health Division. The women were students at various schools (laboratory technicians, nurses, physiotherapy technicians, etc.). Each group was a new one, and most of the persons had spent the previous years in Zürich (40%) or within a radius of about 100 km of Zürich. Each subject was questioned concerning his occupation, sports activity, training, diet, daily intake of milk and milk products and all places of residence.

After a short check on superficial activity of the head, hands and forearms, a shower was taken by the subject before dressing in paper pyjamas. Height and weight were measured and the average perimeter $\overline{P}$ of the trunk determined. The subject was then seated in the chair, care being taken that there was good body contact along the whole profile of the chair. The hands

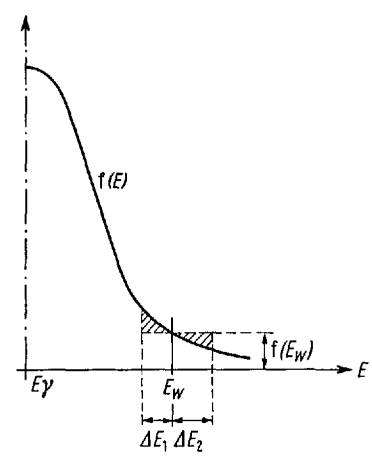

Fig. 15. Schematic diagram of the 2 energy bands ΔE_1 and ΔE_2 taken at the limits E_w of photopeaks of low activity.

[34] The window width for different energies is determined according to the new formula developed recently by T. T. MERCER, Hlth Phys. *12*, 533 (1966): $\bar{\sigma}$ (keV) = 7.90 E_γ (MeV) + 20.3 $\sqrt{E_\gamma}$ (MeV) for a 3 × 3 inch crystal.

were placed under the thighs the elbows sustained 5 cm above the profile. The reproducibility of the crystal-detector position was assured within 2 mm by a removable, horizontal and circular perspex plate mounted on the framework of the chair. (Anti-claustrophobial measures were taken by means of interphone and music. The temperature of the steel room was stabilized at 27.5 °C.)

From the 6 groups measured we analyze below the results of the 2 groups of 50 men and 50 women measured in autumn 1966.

The distribution of the concentration of potassium/kg weight against the *average perimeter* $\overline{P}$ is given in Figure 16 for a group of 50 soldiers. In Figure 17 the distribution of the potassium concentration is given as a function of height of the subject and in Figure 18 as a function of weight. It is seen that in all 3 distributions the *concentration of potassium is independent of the variables $\overline{P}$, height and weight.* This is the result of the crystal-chair geometry used for the measurement. For this group the average concentration amounts to 2.15 g K/kg with a standard deviation of 0.11. Thus the normal variation for 95% of the cases does not exceed 10.5%.

RUNDO, followed by MENEELY et al.[35] and MARINELLI[36], introduced as a check on the self-attenuation effect, an *average thickness* of the body defined by (weight:height)$^{1/2}$. These authors have noted the considerable variation of the calibration from this average thickness and RUNDO[37] made the same observation with his multi-crystal array.

If, for the same group of young men, we plot the potassium concentration against the same variable (weight:height)$^{1/2}$ in the new chair geometry, we obtain the result in Figure 19. We see again that the concentration, on the average, no longer depends on this 'average thickness'[38].

The distribution of the concentration of potassium/kg weight plotted against perimeter $\overline{P}$ for the group of 50 young women of autumn 1966 is given in Figure 20. Similar results were obtained for the concentration of potassium plotted against weight or height. It is again clear that the concentration is independent of the 3

[35] G. R. MENEELY, Circulation Res. *11*, 539 (1962).

[36] L. D. MARINELLI, Argonne National Laboratory Report ANL-7220, 31 (1965–66).

[37] J. RUNDO, Proc. 2nd Int. Conf. peaceful Uses atom. Energy *23*, 101 (1958).

[38] According to our experience, the 'average thickness' is not the best factor to disclose the influence of body shape on calibration. The main part of radioactivity being accumulated in the trunk and thighs, the average perimeter $\overline{P}$ is a more sensitive parameter.

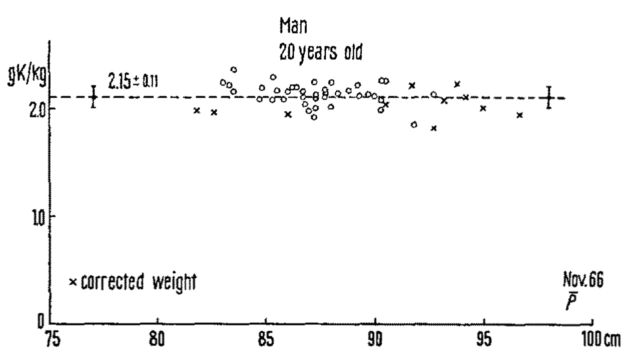

Fig. 16. Potassium concentrations in g/kg plotted against the average perimeter $\overline{P}$. 50 men of age 20 ± 2 years.

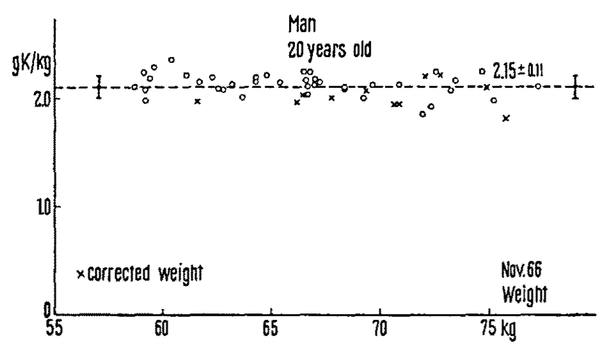

Fig. 18. Potassium concentrations in g/kg plotted against the weight. 50 men of age 20 ± 2 years.

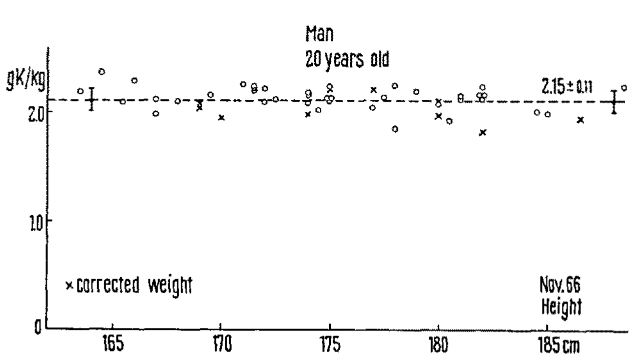

Fig. 17. Potassium concentrations in g/kg plotted against the height. 50 men of age 20 ± 2 years.

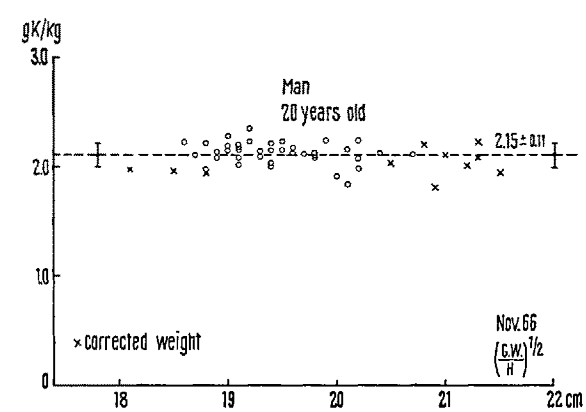

Fig. 19. Potassium concentrations in g/kg versus 'average thickness' in the new 'elliptical' chair geometry. 50 men of age 20 ± 2 years.

variables, just as it is for the 'average thickness' defined by MENEELY. For this group the average concentration is 1.56 g K/kg with a standard deviation of 0.13. Thus, the normal variation for 95% of the cases does not exceed ±17%.

What we have described for the 2 groups measured in autumn 1966 is equally valid for the 4 groups measured in the spring of 1966 and 1967. For all groups the mean potassium concentration/kg weight appears to be independent of the 4 variables $\bar{P}$, height, weight and 'average thickness'.

Table IV gives a summary of the composition of the groups with the average height and weight and the results of the average potassium concentration.

Since the standard deviation from the mean value (standard error) of the potassium concentration in each group is 0.02, the reproducibility of the values may be considered for both to be very good, the more so because each group is always formed with different persons. Thus the average potassium concentration of young men and young women 20 ± 2 years old is well defined and amounts to: young man **2.14 ± 0.02** g K/kg; young woman **1.58 ± 0.02** g K/kg.

It is striking to see that the concentration of potassium in women is about a quarter lower – exactly 26% – than that of the men.

In order to elucidate this difference, with the help of Prof. Dr. med. E. UEHLINGER, Director of the Institute of Pathological Anatomy of the University of Zürich, we measured the ^{40}K activity of striated muscle of the thigh, fresh from dissection. Disk-shaped samples of 60–100 g weight are put in a perspex cylinder 7.5 cm diameter and pressed with a piston on the under face of the crystal in the steel room. Recording over a period of 450 min during the night gives a spectrum as shown in Figure 21. The calibration, being dependent on the tickness of the active layer, is carried out with layers of KCl of different weights put into the cylinder. The results of the measurements, with those of the ^{137}Cs concentration, are given in Table V with their standard error.

Thus the concentration in a woman's muscle appears as 12.5% lower for potassium and 27.5% lower for ^{137}Cs than that in a man's muscle. The difference for potassium is not statistically ascertained; but it is better

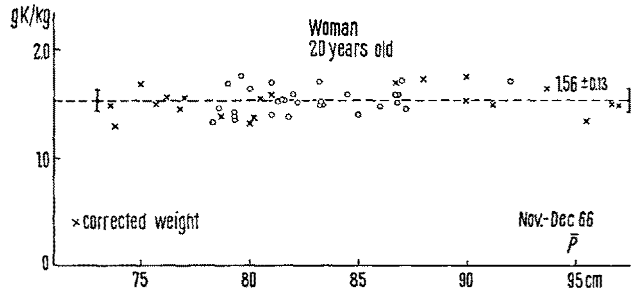

Fig. 20. Potassium concentrations in g/kg versus average perimeter $\bar{P}$. 50 girls of age 20 ± 2 years.

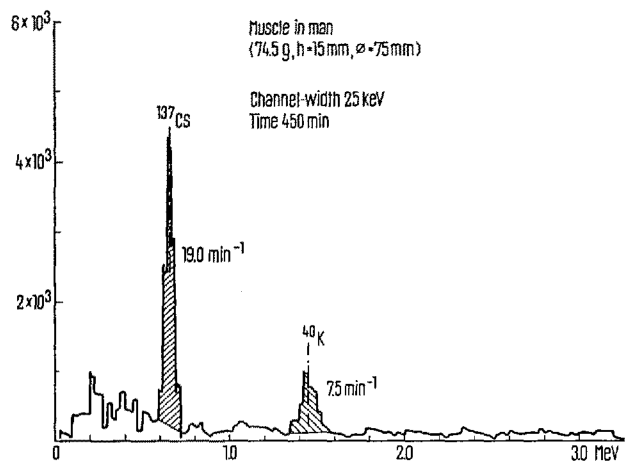

Fig. 21. Spectrum of muscle (fresh from dissection) in man, spring 1965.

Table IV.

Period of measurement	Composition of the groups: Total No.	Distribution in age: 18 (years)	19	20	21	22	Average weight (kg)	Average height (cm)	Potassium concentration g K/kg ± S.D.
		Young men							
Feb. to March 66	45	–	1	39	5	–	66.4	174.7	2.14 ± 0.14
Oct. to Nov. 66	50	1	5	34	8	2	67.1	175.1	2.15 ± 0.11
March 67	51	–	–	47	2	2	65.8	173.4	2.12 ± 0.15
		Young women							
March to May 66	45	–	13	16	12	4	57.9	163.3	1.57 ± 0.14
Nov. to Dec. 66	50	2	23	18	6	1	57.7	163.3	1.56 ± 0.13
May to June 67	53	–	21	19	13	–	57.9	164.9	1.62 ± 0.13

ascertained for ^{137}Cs and may also be considered as probable for both elements.

In Table VI we compare the results obtained by other authors for potassium concentration in the normal man and woman. As many other authors did not initially take account of the difference between man and woman or the influence of age, we are giving the results only where these differences are observed. The figures for 20-year-old persons are underlined.

From the year 1959 we see that our value of 2.14 ± 0.02 for the 20-year-old man agrees very well with those obtained earlier by McNeill et al.[39], Anderson and Langham[5], Wenger and Soucas[40]. The value of Oberhausen et al.[41] is a few % higher. For the 20-year-old woman, however, our figure of 1.58 ± 0.02 agrees well with that of Wenger and Soucas, but is nearly 10% lower than those of Anderson et al. and Oberhausen et al. We do not know the origin of this difference but must stress that our 3 different sets of measurements of females gave consistent results.

It is interesting to note that the first measurements of potassium performed with high-pressure ionization chambers in somewhat complicated conditions with very long counting times agree quite well with the more exact later values. Sievert[2] discovered the influence of sex on K concentration.

The influence of age and fat on potassium concentration, diagnostic application

In 1957, Anderson[42] determined the so-called 'lean body weight' after measurement of the water content of the body with the tritium method (assuming a water concentration of 20% in fat and 72% of basic lean body weight). His conclusion was that the potassium content of the fat-free weight was 0.28% and appeared independent of weight, age and sex. In a later publication with Langham[5] in 1959, he gave the dependence of age and 'gross body weight' for 1590 subjects of ages varying from 1–79 years. The results of these investigations are summarized in Figure 22. The maximum concentration occurs at 9 years of age in the female and at 16 years in the male. Between the ages of 20 and 60 a net loss in males was 18% without variation of the gross weight. In females, after correction for increase in gross body weight with increasing age, the decrease in concentration was only about 6%.

[39] K. G. McNeill and R. M. Green, Can. J. Phys. *37*, 683 (1959).
[40] P. Wenger and K. Soucas, Helv. chim. Acta *47*, 947 (1964).
[41] E. Oberhausen, W. Burmeister and E. J. Huycke, Annls paediat. *205*, 381 (1965).
[42] E. C. Anderson, Br. J. Radiol., Suppl. *7*, 27 (1957).

Table V. Concentration of potassium in muscle

Striated muscle	Samples	Potassium g K/kg	^{137}Cs nCi/kg
Man	17	4.04 ± 0.22	0.87 ± 0.11
Woman	11	3.53 ± 0.30	0.63 ± 0.08

Table VI. Potassium concentration in young man and woman

Author	Year	Device	Man			Woman		
			No.	Age	g K/kg	No.	Age	g K/kg
Burch[3]	1954	High pressure	11	20–41	2.12 ± 0.1	–	–	–
Rundo[4]	1955	ionization	6	22–31	2.15 ± 1.2	4	17–28	1.97 ± 1.5
Sievert and Hulquist[2]	1956–57	chambers	11	20–29	$1.9_6 \pm 0.1_0$	4	25–28	1.45 ± 0.05
Marinelli[8]	1956	1 NaI (Tl) crystal	12	22–34	$1.8_8 \pm 0.06$	3	22–29	1.54 ± 0.03
Anderson[42]	1956	4π-Liquid scintillator	28	–	2.1_0	16	–	1.60
McNeill and Green[39]	1959	1 NaI (Tl) crystal	30	~20	$2.1_2 \pm 0.1_3$	–	–	–
Anderson and Langham[5]	1959	4π-Liquid scintillator	Large	20	2.13 ± 0.05	Large	20	1.73 ± 0.05
Wenger and Soucas[40]	1964	1 NaI (Tl) crystal	20	18–30	2.06 ± 0.08	18	18–30	1.63 ± 0.10
Oberhausen et. al.[41]	1965	2π-Liquid scintillator	159	20	2.20 ± 0.02	115	20	1.71 ± 0.02
This paper	1967	1 NaI (Tl) crystal	146	20	2.14 ± 0.02	147	20	1.58 ± 0.02

We found a somewhat similar variation of the potassium concentration as a function of age in the measurement of only 33 normal males. The results are given in Table VII.

But as a correction of the gross weight was obviously necessary for some adipose men, we do not view with full confidence these results. It seems necessary, in each case, to make a separate *determination of the weight of fat.* For diagnostic work especially, the assumption of a constant potassium concentration/kg lean body weight is no longer acceptable because this concentration itself varies with the pathological situation.

In our groups of 20-year-old subjects, twice the standard deviation from the mean ($\bar{P} = 0.05$) amounts to 16% for the woman and 12% for the man. These variations are low in contrast to other groups of determinations. However, they are still too great for the determination of systematic differences involved in physical training or slight pathological anomalies.

Table VIII gives the results of repeated measurements of the total potassium weight on 8 men and 8 women of different ages. The measurements were made at intervals of about 4 months. The extreme variations of the gross weight are quoted.

Table VII. The influence of age on potassium concentration

No.	Age	g K/kg
146	20	2.14 ± 0.02
13	25–34	1.89 ± 0.07
13	35–44	1.94 ± 0.10
7	> 45	1.82 ± 0.06

In one female* the potassium weight was reduced by pregnancy and in a second** through application of steroid hormones. In all cases where the extreme variations were higher than 2 σ (higher than 12–14%) a physiological modification can be suspected. Here we clearly see the importance of improving precision.

For the measurement of fat, B. FRANÇOIS[43,44] has recently carried out extensive research concerning different methods such as tritium dilution in normal man, ratio of body and bone circumferences, and measurement of different skinfolds. According to his

[43] B. FRANÇOIS and R. JOLY, Minerva nefrol. *13*, 1 (1966).
[44] B. FRANÇOIS, Cah. méd. lyonnais *43*, 183 (1967).

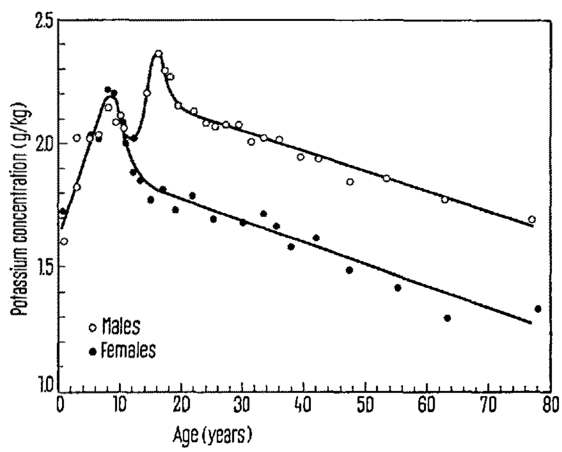

Fig. 22. Potassium concentration in g/kg versus age, according to ANDERSON and LANGHAM[5].

Table VIII. Reproducibility of potassium measurements

Case	Age	Height (cm)	Gross weight (kg)	Total g K 1.	2.	3.	4.	Extremes variations (%)
Women								
B.A.	26	167	56.9–59.2	98	106	100	89	17
F.V.	19	162	54.8–58.6	80	89	85	86	11
G.U.	23	159	53.0–55.0	91	76	68*	83	18
J.M.-L.	43	169	52.1–55.2	86	90	89	74**	4.5
M.M.	42	177	62.2–64.3	98	97	108	97	11
O.U.	20	169	55.8–57.1	85	80	86	91	13
V.H.	41	156	55.3–57.3	110	96	98	89	21
W.I.	21	166	55.4–59.6	96	99	103	104	8
Men								
B.R.	20	178	69.8–78.7	148	158	146	146	8
F.W.	20	180	82.0–85.2	145	134	146	140	9
H.A.	39	173	70.2–73.1	127	–	127	130	2.3
J.G.	62	190	85.5–87.3	143	133	134	138	7.3
M.R.	40	171	70.5–71.6	146	139	156	130	18
M.A.	20	174	66.7–68.9	150	146	151	133	12
R.M.	20	178	71.1–72.0	150	137	140	152	10
V.W.	43	168	57.0–58.3	136	124	123	134	10

comparison, it seems that the percentage of fat in the weight may be determined with reasonable precision with the rather simple method of the skinfolds.

With these 2 improvements, measurement of fat percentage and gain in statistical precision, it seems that the measurement of potassium concentration in lean body weight will be very useful in solving some problems such as influence of physical training and diagnostic research.

According to the experience we have acquired thus far in the various clinics of the University Hospital, a deviation of the total body potassium may occur in the following cases:

Hyperaldesteronismus or Conn-syndrom;

Muscular dystrophy and myotonia atrophica, BLAHD et al.[45];

Influence of oestrogen and gravidity;

Influence of diuretica, cortison and praegdison.

Further, ALLEN et al.[46] found a strong correlation between *basal metabolic rate* (BMR) and total-body potassium, each increasing g of potassium being associated with an increasing heat output of 8.03 kcal/day. The equation for a least squares fit to these data is

$$\mathrm{BMR} \cdot (\mathrm{kcal/day}) = 13.3 + 8.03\ \mathrm{K}\ (\mathrm{g}).$$

This equation seems to apply to both male and female adults and, perhaps, even to children.

All these medical applications of total potassium measurements are to be developed in collaboration with members of the clinical staff of the Kantonsspital of Zürich.

Conclusions. (1) In order to develop a multi-purpose whole-body spectrometer to be used for the checking of professional exposure, for the control of the population at large, and for diagnostic work, we built a steel room equipped with a standard integral line NaI (Tl)-crystal 8 × 4 inches, connected to a RCL 256-channel analyzer. Thus the lower sensitivity but higher resolution of a crystal was preferred to the higher sensitivity but poorer resolution of an organic 2π- or 4π-scintillator.

(2) The reduction of the background between 0.1 and 1.5 MeV, with a steel thickness of 18 cm, a lead coating of 3 mm, positive air-pressure with transit time of 5 min, amounts to a factor of 110. The activity per cm^3 of crystal is 0.26 min^{-1} in the 0.1–2.0 MeV energy range and the in vivo spectrometric resolution is 9.2% for ^{137}Cs. The net background under the 250 keV energy band of ^{40}K (coming chiefly from the phototubes) reaches 59 min^{-1}. One sees that the limits of reduction of the background would be obtained with a steel-thickness of 24 cm and inactive phototubes, the 'background index' then would be reduced to about 0.18 min^{-1}/cm^3 crystal.

(3) The first measurements of 37 men in a standard tilting chair geometry showed strong dependency of the apparent ^{40}K concentration on the average circumference of the trunk. The problem of the self-attenuation and geometry of a thick radioactive layer was studied theoretically and could be experimentally confirmed with phantoms of sections of the trunk. The relative activity $\boldsymbol{M}$ per unit weight is related to the absolute specific activity A by the equation

$$\boldsymbol{M} = A \cdot \boldsymbol{G}_p \cdot \boldsymbol{A}_a .$$

The *self-attenuation factor* $\boldsymbol{A}_a$ may be maintained almost constant for a certain range of layer thickness by good selection of the distance to the crystal (balancing the γ-self-attenuation by the inverse-square law of distance). This distance was 57 cm on the axis of the crystal for ^{137}Cs and ^{40}K. The *geometry factor* $\boldsymbol{G}_p$ is similarly constant if the profile of the chair gives a constant answer in the photopeak for a γ-point source. Both conditions are realized in the energy range of 0.4 up to 1.5 MeV if the profile of the chair is nearly elliptical with a vertical half axis of 62 cm and a horizontal one of 50 cm (from the crystal center).

(4) An articulated *phantom* of the standard man (using up to 18 pieces and filled with KCl-solution) placed in the new chair gives for each piece (abdomen, pelvis, thighs, head etc.) a constant response ± 2% in the photopeak/g solution. Assembling with this phantom 4–5 types of men with an average trunk perimeter varying from 83.6 up to 103.2 cm and 161–179 cm tall, we obtained almost constant calibration factors of $0.43_5 \pm 0.01_2$ min^{-1}/g K, $5.59 \pm 0.1_9$ min^{-1}/nCi ^{137}Cs and $5.75 \pm 0.2_4$ min^{-1}/nCi ^{131}I.

(5) The measurement of the ^{40}K activities in the new chair of 6 groups of normal persons, each group including about 50 young men or young women 20 years old, gave an average potassium concentration of 2.14 ± 0.02 (S.E.) g/kg for the man and 1.58 ± 0.02 g/kg for the woman. Plotting the individual potassium concentration against the average trunk perimeter, the body weight, the height, or the usual variable (weight to $\mathrm{height})^{1/2}$, the K concentration appears to be practically independent of these 4 variables. In the new chair-crystal geometry (for γ-energies of 0.4–1.5 MeV), if the distribution of the radioactivity is homogeneous, the relative specific activity in the photopeak/kg weight is practically independent of body shape and size.

(6) With a measuring time of 45 min, the overall standard deviation of repeated measurements of K-concentration on a group of 18 persons is about 7.5%. This somewhat high value could be reduced to roughly

[45] W. H. BLAHD, B. CASSEN, M. LEDERER and E. J. DRENICK, in *Clinical Uses of Whole-Body Counting* (International Atomic Energy Agency, Vienna 1966), p. 169.

[46] T. H. ALLEN, E. C. ANDERSON and W. H. LANGHAM, J. Geront. *15*, 348 (1960).

3% by 3 improvements, namely a determination of fat percentage of each person for calculation of the lean body weight, the use of a larger crystal (e.g. 13 × 7 inches), and a further reduction of the background in the ^{40}K window through the use of inactive phototubes. The excellent reproducibility obtained for many measurements on the same subject with 4π- or 2π-counters (46, 41, 5) indicate that the K-concentration/kg lean body weight should be a constant, which is modified only by precise causes such as physical training or pathological situations[47].

Résumé. Les avantages d'un spectromètre à chambre d'acier avec grand monocristal de NaI (Tl) sont tout d'abord comparés à ceux d'un spectromètre à paires de cristaux, mobiles ou fixes (multipaires), ou à scintillateurs organiques avec angle solide de 2 ou 4 π. Pour des applications variées: contrôle de l'exposition professionnelle, de l'activité de la population générale et pour le diagnostic médical, le spectromètre à grand cristal (on peut aller jusqu'a 35 cm de diamêtre et 18 cm de hauteur), à pouvoir séparateur élevé, est à préférer à la grande sensibilité mais à la mauvaise résolution des scintillateurs organiques.

L'analyse des différentes étapes de la réduction du «background», avec un écran d'acier de 18 cm d'épaisseur, montre que l'abaissement maximum peut être obtenu avec 24 cm d'acier et des photomultiplicateurs inactifs («background index» de 0,18 min^{-1} cm^{-3} de 0,1–2,0 MeV pour le cristal de 8″ × 4″).

Les premières mesures de ^{40}K, effectuées dans le fauteuil standard préconisé par le Laboratoire de l'Argonne, ayant confirmé la variation élevée de l'étalonnage en fonction du pourtour moyen du tronc, le problème de l'auto-atténuation gamma dans le corps humain et celui de la géométrie cristal-sujet ont été systématiquement étudiés. On montre que lorsque l'épaisseur du corps varie, la variation de l'auto-atténuation γ peut être pratiquement compensée – de 0,4–1,5 MeV – pour une répartition homogène, par la variation du carré de la distance au cristal. Le profil du fauteuil doit alors être quasi-elliptique (réponse constante sous le «photopeak» dans un plan de symétrie vertical pour une source ponctuelle de 1,33 ou 0,662 MeV) avec un demi-axe vertical de 62 cm et un demi-axe horizontal de 50 cm.

Dans cette géométrie, les mesures de 6 groupes de 50 sujets de 20 ans nous ont montré que la concentration moyenne de potassium est indépendante du périmètre moyen du tronc, du poids, de la taille et de la grandeur (poids: taille)$^{1/2}$. La concentration moyenne est de 2,14 ± 0,02 (S.E.) pour l'homme et de 1,58 ± 0,02 g K/kg de poids pour la jeune fille.

La même géométrie cristal-sujet est sans autre applicable – avec une légère correction pour les variations du rapport photo: total – à la mesure de radioéléments à répartition non homogène tels que le ^{47}Ca ou le ^{85}Sr.

[47] Gauger & Co. in Zürich built the steel room with old steel manufactured by von Roll in Gerlafingen. Ing. H. Weiss and J. Scherrer Söhne, Zürich, carried out the inner equipment.

SPECIALIA

The Syntheses of Centaureidin and 5,7,3′-Trihydroxy-3,8,4′-trimethoxyflavone

Centaurein (I) was isolated from roots of *Centaurea jacea* L. by BRIDEL et al.[1], its hydrolysis (I) with sulphuric acid afforded centaureidin (II). FARKAS et al.[2] established the structure of II to be 5,7,3′-trihydroxy-3,6,4′-trimethoxyflavone. Recently, II have also been isolated from the *Centaurea* species by BOHLMANN et al.[3]. II is a structural isomer of jaceidin (III), which has been isolated from the same plant[3,4] and synthesized by the present author[5]. This paper describes syntheses of II and 5,7,3′-trihydroxy-3,8,4′-trimethoxyflavone (IV), an isomer of II, from 2,4,6-trihydroxy-3,ω-dimethoxyacetophenone (V) according to a modified procedure reported earlier[5,6].

Allan-Robinson's reaction of keton V with *O*-benzylisovanillic anhydride and potassium *O*-benzylisovanillate was expected to afford 2 isomeric cyclization products VI and VII. The isolation of both products at this stage was eventually not accomplished. The flavone VI [m.p. 163–164°, UV λ_{max}^{EtOH} nm (log ε): 255 (4.28), 272 (4.21), 348 (4.34). Found: C, 66.41; H, 4.90. $C_{25}H_{22}O_8$ requires: C, 66.66; H, 4.92%] and the flavone VII, an isomer of VI [m.p. 148–149°, UV λ_{max}^{EtOH} nm (log ε): 257.5 (4.30), 276 (4.27), 340 (4.20), 362_{sh} (4.20). Found: C, 66.61; H, 4.91. $C_{25}H_{22}O_8$ requires: C, 66.66; H, 4.92%] were obtained only after purification via acetylation, followed by hydrolysis. Catalytic hydrogenolysis of VI over palladium charcoal yielded the desired flavone II [m.p. 196–197°, UV λ_{max}^{EtOH} nm (log ε): 257 (4.29), 271 (4.22), 293 (3.99), 351 (4.32). Found: C, 59.79; H, 4.35. $C_{18}H_{16}O_8$ requires: C, 60.00; H, 4.48%) (lit.[2] m.p. 196°) (triacetate: m.p. 174–175.5°, UV λ_{max}^{EtOH} nm (log ε): 328 (4.00), 344 (4.06)]. Ethylation of II by the usual method gave 5,7,3′-triethoxy-3,6,4′-